Springer

Journal of
Mechanical
Science and
Technology

Journal of Mechanical Science and Technology 22 (2008) 812~818

www.springerlink.com/content/1738-494x

A Granular motion simulation by discrete element method

Yu-Man Kim*

Linkworks, Business Incubating Center 310, Hankook University of Foreign Studies, 449-791 Wangsan-ri Mohyeon-myeon Cheoin-gu Yongin-shi Gyeonggi-do Korea

(Manuscript Received August 28, 2007; Revised January 9, 2008; Accepted January 11, 2008)

Abstract

A granular system is defined as a group of tiny particles; they interact with each other by collisions and elastic force. To analyze granular dynamics, conventional methods based on continuum mechanics are not applicable, so new simulation methods are needed. Recently, thanks to improvement in computing technology, the discrete element method (DEM) is being focused on, in which equations of motion are built on each particle and the behavior of all particles is analyzed by solving those equations. In this paper, a computer program has been developed to analyze particle dynamics by using the discrete element method. As examples, the particle packing process and mono-component non-contact development process in a laser printer are simulated. It is seen that the particle motions in the processes are well described by the program.

Keywords: Granular system; Discrete element method; Particle packing process; Development process; Toner particle; Laser printer

1. Introduction

A granular system, originally a group of discrete solid particles, cannot be treated as a continuum. Thus, conventional tools such as finite element methods (FEM) are not applicable to analyze the behavior of the particles. In the late 1950s, molecular dynamics (MD) in computational physics was developed, and Alder analyzed phase transition of iron[1]. In MD, the motion of each particle is computed by solving the equation of motion derived from Newton's 2nd law. Based on this concept, Cundall developed the distinct element method and analyzed the behavior of soil in civil engineering[2]. By virtue of advances in computing technology, it has been modified and improved and called by the name of discrete element method (DEM). In the printer industry, specifically for laser printers, the behavior of toner particles was studied. Nakano simulated the toner motion in the development process[3], and Kadonaga studied the transfer process using DEM[4]. In order to simulate large numbers of particles, parallel computing was used in DEM[5].

In this paper, a 2-dimensional DEM program is developed, and as model cases, two processes of particle packing and mono component non-contact development processes are simulated. As a result, the trajectories of particle motion are calculated and plotted.

2. Formulation

2.1 Discrete element method

When a group of particles are moving, the individual particle is affected by contacting particles as shown in Fig. 1. Once the contact forces on a particle are known, according to Newton's 2nd law of motion, acceleration of the particle is determined and the velocity and displacement are obtained by time integration. Applying this process to all the particles, motions of all particles can be analyzed.

In order to establish the equation of motion of the particle, the contact force is decomposed into two components, normal and tangential directions. For

*Corresponding author. Tel.: +82 502 698 4123
E-mail address: yumann_kim@naver.com
DOI 10.1007/s12206-008-0112-7

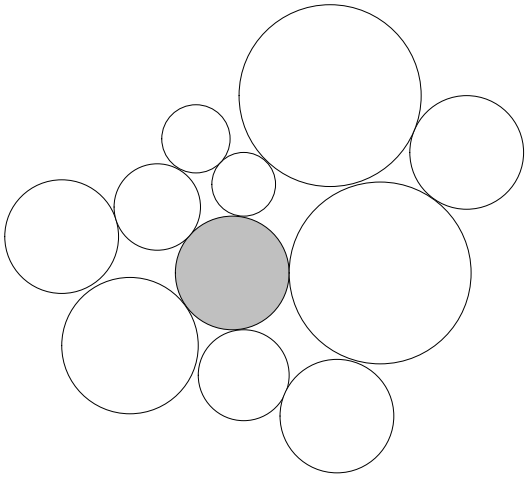

(a)

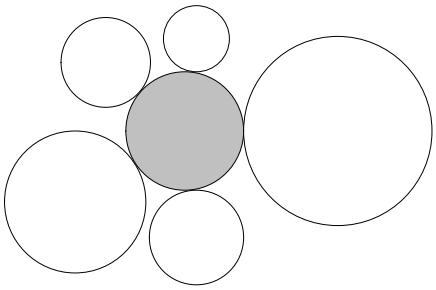

(b)

Fig. 1. (a) A group of particles are moving. (b) One particle of interest is in contact with adjacent particles.

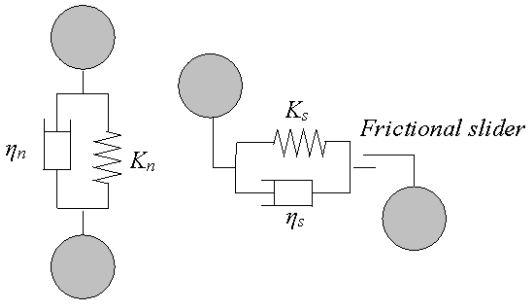

(a) (b)

Fig. 2. Voigt contact model of two particles for (a) normal and (b) tangential directions.

each direction, we apply the Voigt model, in which the elastic and damping forces are involved and the large frictional reaction is considered as a frictional slider as shown in Fig. 2. The equation of motion is expressed as

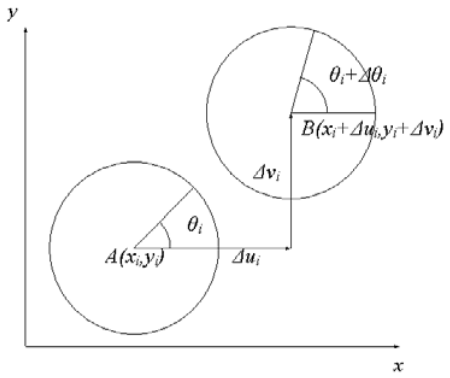

Fig. 3. Translational and rotational displacements of a particle in the time interval of Δt.

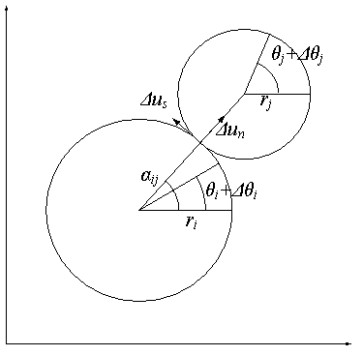

Fig. 4. Normal and tangential increments of displacement when the two particles are in contact.

$$m\frac{d^2u}{dt^2}+\eta_n\frac{du}{dt}+K_nu=0 \tag{1}$$

$$J\frac{d^2\theta}{dt^2}+\eta_s\frac{d\theta}{dt}+K_s\theta=0 \tag{2}$$

for translational and rotational motions, respectively, where, u and θ are the displacement vector and rotation of the particle, m and J are mass and moment of inertia, K and η are the elastic and damping coefficients of two particles in contact. The lowercase letters n and s denote the normal and tangential directions, respectively.

2.2 Relative displacement increments

As shown in Figs. 3 and 4, when the i-th particle moves from the point A to B during time increment Δt, it is expressed as Δu_i and Δv_i which are the x and y components of the displacement increment of the particle, respectively. $\Delta\theta_i$ denotes the rotational increment. Two particles with radius r_i and r_j are in contact with each other when satisfying

$$r_i + r_j \geq L_{ij} \tag{3}$$

where L_{ij} is the distance of centers of the two particles, defined as

$$L_{ij} = \sqrt{(x_i - x_j)^2 + (y_i - y_j)^2}\,. \tag{4}$$

The contact position of the two particles can be determined by using the angle α_{ij} between two lines, the normal line joining the center points and the x axis

$$\sin\alpha_{ij} = \frac{y_j - y_i}{L_{ij}},\quad \cos\alpha_{ij} = \frac{x_j - x_i}{L_{ij}}\,. \tag{5}$$

Hence, the normal and tangential components of the relative displacement increment in contacting two particles are expressed as

$$\Delta u_n = (\Delta u_i - \Delta u_j)\cos\alpha_{ij} + (\Delta v_i - \Delta v_j)\sin\alpha_{ij}\,, \tag{6}$$

$$\Delta u_s = -(\Delta u_i - \Delta u_j)\sin\alpha_{ij} + (\Delta v_i - \Delta v_j)\cos\alpha_{ij} + (r_i\Delta\theta_i + r_j\Delta\theta_j)\,. \tag{7}$$

2.3 Contact forces

During the time increment Δt, the contact forces acting on the particles are expressed as

$$\Delta e_n = K_n \Delta u_n\ ,\ \Delta d_n = \eta_n \frac{\Delta u_n}{\Delta t} \tag{8),(9}$$

for elastic and damping forces of normal direction respectively. Therefore, at time t, the normal component of contact force is

$$[f_n]_t = [e_n]_t + [d_n]_t \tag{10}$$

where

$$[e_n]_t = [e_n]_{t-\Delta t} + \Delta e_n\,,\quad [d_n]_t = \Delta d_n\ . \tag{11),(12}$$

Similarly, for tangential direction, the elastic and damping forces are

$$\Delta e_s = K_s \Delta u_s\ \ ,\ \ \Delta d_s = \eta_s \frac{\Delta u_s}{\Delta t} \tag{13),(14}$$

and

$$[f_s]_t = [e_s]_t + [d_s]_t \tag{15}$$

where

$$[e_s]_t = [e_s]_{t-\Delta t} + \Delta e_s\,,\quad [d_s]_t = \Delta d_s\ . \tag{16),(17}$$

Considering the frictional slider, according to Coulomb's law of friction, the following conditions are added:

$$[e_s]_t = [d_s]_t = 0 \ \text{ when } \quad [e_n]_t \leq 0 \tag{18}$$

and

$$[e_s]_t = \mu[e_n]_t\, sign([e_s]_t)\,,\quad [d_s]_t = 0$$

when $[e_s]_t \geq \mu[e_n]_t$, (19)

where μ is the friction coefficient.

2.4 Acceleration, velocity and displacement

Total force and moment acting on the particle i can be expressed as follows:

$$[X_i]_t = \sum_j \{-[f_n]_t \cos\alpha_{ij} + [f_s]_t \sin\alpha_{ij}\} + m_i g_x \tag{20}$$

$$[Y_i]_t = \sum_j \{-[f_n]_t \sin\alpha_{ij} - [f_s]_t \cos\alpha_{ij}\} + m_i g_y \tag{21}$$

$$[M_i]_t = -r_i \sum_j [f_s]_t \tag{22}$$

where g_x and g_y are x and y components of accelerations due to external forces such as gravitational or electric forces. Summation on j means the total contact force by particles in contact with the particle i. Therefore, the translational and rotational accelerations are

$$[a_{xi}]_t = [X_i]_t / m_i \tag{23}$$

$$[a_{yi}]_t = [Y_i]_t / m_i \tag{24}$$

$$[\alpha_i]_t = [M_i]_t / J_i\,. \tag{25}$$

By time integration, the velocity and displacement of the particle are derived from the above accelerations.

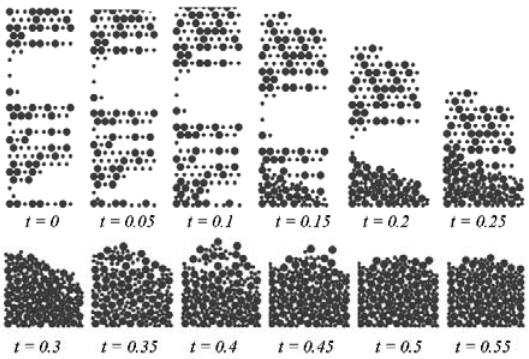

Fig. 5. Snapshots of the particle packing process as a result of simulation.

Table 1. Parameters used in particle packing process simulation

Parameters	Values
Young's modulus of particle	4.9×10^9 [Pa]
Young's modulus of wall	3.9×10^9 [Pa]
Poisson ratio of particle	0.23
Poisson ratio of wall	0.25
Radius of particle	0.01, 0.005 [m]
Friction coefficient (particle to particle)	0.25
Friction coefficient (particle to wall)	0.17
Density of particle	2.5×10^3 [kg/m^3]
Number of particle	149
Time increment	2.5×10^{-6} [s]
Width of vessel	0.2 [m]

2.5 Determination of the elastic and damping coefficients

The elastic coefficient for normal direction is determined according to Hertzian contact theory[6],

$$K_n = A(F\Delta)^{1/3} / \gamma \tag{26}$$

where A is a proportional constant, F is the contact force for normal direction, and

$$\Delta = \gamma \frac{r_i r_j}{r_i + r_j} \quad , \quad \gamma = \frac{1-\nu_i^2}{E_i} + \frac{1-\nu_j^2}{E_j} \tag{27),(28}$$

where E and ν are Young's modulus and Poisson ratio respectively.

For the tangential direction, the elastic coefficient is obtained by multiplying K_n and the ratio of shear and Young's modulus[7]:

$$K_s = \frac{G}{E} K_n \tag{29}$$

where G is shear modulus of the particle.

The damping coefficients are determined by the critical damping condition from Eqs. (1) and (2):

$$\eta_n = 2\sqrt{mK_n} \quad , \quad \eta_s = 2\sqrt{mK_s} \quad . \tag{30),(31}$$

3. Simulation

3.1 Particle packing process

The particle packing process has been chosen as a typical example to test DEM algorithms[8]. This process means that a vessel is filled with particles under gravitational force. In Table 1, the parameters used in simulation are listed. The process is simulated up to 0.55s with the time increment 2.5μs. As a result of simulation, a series of snapshots of the moving particles are shown in Fig. 5. It is seen that the motion of the particles is well described.

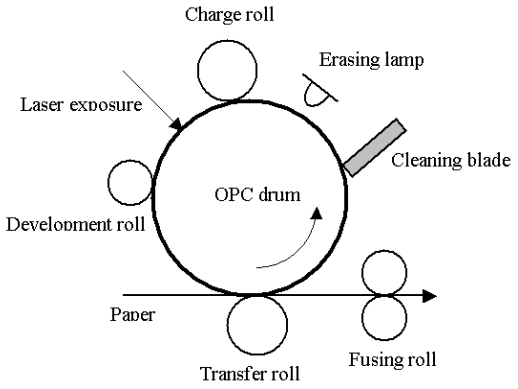

Fig. 6. Schematic diagram of the printing processes in laser printers.

3.2 Non-contact development process

The printing processes in laser printers are depicted in Fig. 6. The organic photoconductor(OPC) drum is an electrically grounded aluminum one coated with organic photoconducting material which becomes conductive only when exposed by the light with specific wavelength. The OPC drum is charged up to the charging voltage by a charge roll with the same polarity of toner. By laser exposure, on-off controlled according to the image signal, an electrical latent image is formed on the OPC surface. The exposed area, or image area, retains zero voltage. When the OPC drum goes through the development roll, the charged toner particles on the surface of the development roll begin to move according to the electric field generated between the OPC drum and the development roll. Therefore, the image area is developed by the toner particles. And the toner image on the OPC drum is electrically transferred into the paper by the transfer roll exerted by high voltage with the opposite polarity of the toner. By passing through the fusing rolls, the images on the paper are fixed by high temperature and pressure. After the transfer process, the residual toners on the OPC drum are swept away by

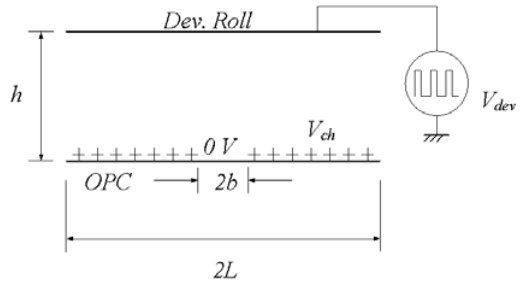

Fig. 7. Configuration of the mono component non-contact development process.

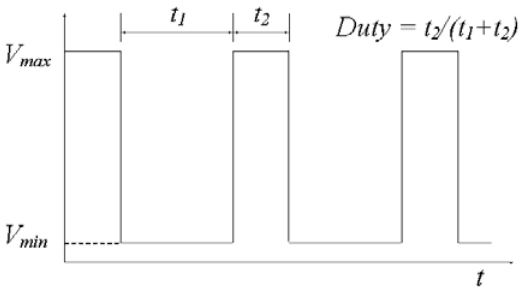

Fig. 8. Waveform of the voltage exerted to development roll.

the cleaning blade. The erasing lamp makes the electrical potential of the OPC surface uniform. "Non-contact development" means that there is a gap between the OPC drum and the development roll.

To find the external force exerted on the toner particles, the electric field in development region should be calculated. Configuration of the development process is depicted in Fig. 7. An alternate voltage is exerted on the development roll, and the surface of the photoconductor has zero potential at the image area. In Figs. 8 and 9, the waveforms of potentials of the development roll and the photoconductor surface are shown. The fluctuation in the surface potential distribution of the photoconductor comes from Fourier series approximation as follows:

$$V_{opc}(x) = a_0 + \sum_{n=1}^{\infty} a_n \cos(\alpha_n x) \tag{32}$$

where, $\alpha_n = \frac{n\pi}{L}$ and

$$a_0 = \frac{(L-2b)}{2L} V_{ch} + \frac{V_{ch}}{2}, \quad a_n = \frac{-2\sin(\alpha_n b)}{\pi n} V_{ch} \tag{33}$$

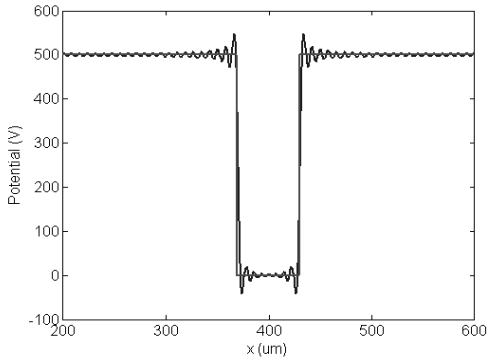

Fig. 9. Potential distribution and its Fourier series approximation on the photoconductor surface.

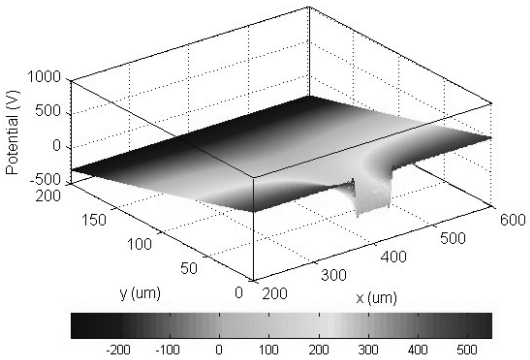

Fig. 10. Potential distribution in the development region when h = 200 μm, b = 30 μm, L = 200 μm, V_{dev} = -300 V and V_{ch} = 500 V.

where, V_{ch} is the potential of the non-image area.

The potential distribution of the development region is expressed as

$$\phi(x,y) = \sum_{n=1}^{\infty} \phi_n \cos(\alpha_n x)(e^{\alpha_n y} + B_n e^{-\alpha_n y}) + p + qy \tag{34}$$

where, the coefficients and constants are given by

$$\phi_n = a_n / (1+B_n) \ , \quad B_n = -e^{2\alpha_n h} \tag{35),(36}$$

and

$$p = a_0 \quad , \quad q = \frac{V_{dev} - p}{h} \ . \tag{37}$$

Therefore, the electric field can be obtained by taking gradient of the potential,

Table 2. Parameters used in non-contact development process simulation.

Parameters	Values
Young's modulus of particle	4.9×10^{6} [Pa]
Young's modulus of wall	3.9×10^{7} [Pa]
Poisson ratio of particle	0.23
Poisson ratio of wall	0.25
Radius of particle	4, 2.5 [um]
Friction coefficient (particle to particle)	2.5×10^{-3}
Friction coefficient (particle to wall)	1.7×10^{-3}
Density of particle	1.1×10^{3} [kg/m^3]
Number of particle	45
Time increment	1.0×10^{-8} [s]
Width of image area	60 [um]
Development gap	200 [um]
Frequency of development voltage	2 [kHz]
Duty of development voltage	0.3
Charging voltage	500 [V]
Exposure voltage	0 [V]
Number of terms for Fourier series	50
Max. development voltage	1200 [V]
Min. development voltage	-300 [V]
Q/M of toner particle	20 [uC/g]

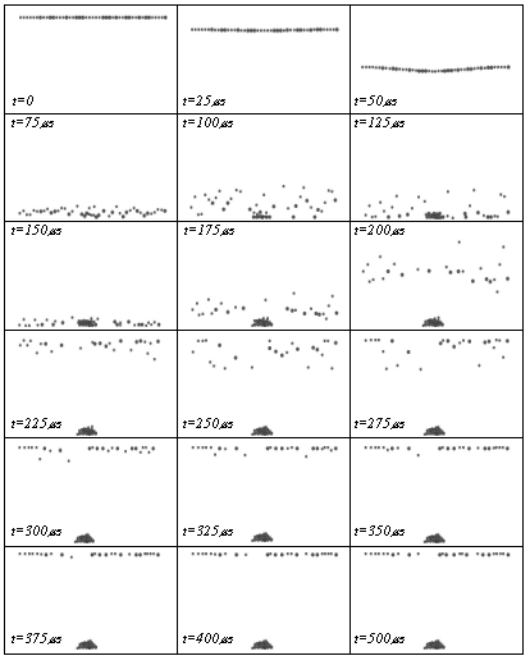

Fig. 11. Snapshots of non-contact development process as a result of simulation.

$$E_x = -\frac{\partial \phi}{\partial x} \quad , \quad E_y = -\frac{\partial \phi}{\partial y} \quad . \tag{38}$$

In Fig. 10, the potential distribution of the development region is shown.

The electric force of a charged particle is calculated by multiplying the particle charge by the electric field. Table 2 lists the parameters used in simulation. In order to suppress rolling of toner particles on the surfaces of the development roll and photoconductor, the friction coefficients are set to very small values.

In Fig. 11, the motions of toner particles are shown during one period (500μs). Initially, the toner particles are located on the surface of the development roll; according to the electric field applied, the particles begin to move and develop the image area of the photoconductor. It is seen that the behavior of toner particles is well described, although only the electric field force as an external force is considered.

4. Conclusion

A computer program simulating the dynamics of particles has been developed based on DEM. To test the program, two cases of particle packing and non-contact development processes are simulated. As a result, the trajectories of all particles are calculated and plotted. It is shown that the behavior of particles is well described. This method is expected to be very useful to simulate the behavior of toner particles in the laser printing process.

For better simulation of a real situation, the program will be improved considering a large number of toner particles with various sizes and charge per mass (Q/M). The air drag force and Coulomb's force between toner particles will be also added in the external forces.

Nomenclature

b : Half length of image area in non-contact development
E : Young's modulus of a particle
E_x : x component of electric field
E_y : y component of electric field
G : Shear modulus of a particle
h : Gap between OPC drum and development roll
J : Moment of inertia of a particle
K : Elastic coefficient
L : Half length of simulation area in non-contact

development
L_{ij} : Distance between centers of the two particles
m : Mass of a particle
r_i : Radius of the i-th particle
u : Displacement vector of a particle
V_{ch} : Surface potential of photoconductor at non-image area
V_{dev} : Potential of development roll
V_{opc} : Surface potential of photoconductor
x_i : x coordinate of the center of the i-th particle
y_i : y coordinate of the center of the i-th particle
$[a_{xi}]_t$: x component of acceleration of the i-th particle at time t
$[a_{yi}]_t$: y component of acceleration of the i-th particle at time t
$[f_n]_t$: Normal component of contact force at time t
$[f_s]_t$: Tangential component of contact force at time t
$[M_i]_t$: Total moment of the i-th particle at time t
$[X_i]_t$: x component of total force of the i-th particle at time t
$[Y_i]_t$: y component of total force of the i-th particle at time t
α_{ij} : Angle between the line joining centers of two contact particles and the x-axis
d_n : Normal component of contact damping force in time increment t
d_s : Tangential component of contact damping force in time increment t
e_n : Normal component of contact elastic force in time increment t
e_s : Tangential component of contact elastic force in time increment t
t : Time increment
u_n : Normal component of displacement increment
u_s : Tangential component of displacement increment
u_i : x component of displacement increment of the i-th particle
v_i : y component of displacement increment of the i-th particle
$\Delta\theta_i$: Rotation increment of the i-th particle
η : Damping coefficient
θ : Rotation of a particle
μ : Frictional coefficient
ν : Poisson's ratio of a particle
φ : Potential distribution in development region
$[\alpha_i]_t$: Angular acceleration of the i-th particle at time t

References

[1] B. J. Alder and T. F. Wainwright, Phase transition for a hard sphere system, *J. Chem. Phys.* 27 (1957) 1208-1209.
[2] P. A. Cundall and O. D. L. Strack, A discrete numerical model for granular assemblies, *Geotechnique* 29 (1979) 47-65.
[3] M. Nakano and I. Itoh, Analysis of toner motion in the development process, Japan Hardcopy 2003, (2003) 261-264.
[4] M. Kadonaga, T. Takahashi and H. Iimura, A study of image degradation in 1st transfer process, Japan Hardcopy 2005, (2005) 103-106.
[5] T. Watanabe, Numerical simulation of carrier behavior around a magnet roll in two component developer unit in electrophotography, IS&T's NIP 21: International Conference on Digital Printing Technologies, (2005) 578-581.
[6] D. P. Walter, Formulas for Stress, Strain and Structural Matrices, John Wiley & Sons, (1994) 403-411.
[7] Buntaikogakkai, Buntai Simulation Nyumon, Sangyotosho, (1998) 29-44.
[8] F. Fleissner, T. Gaugele and P. Eberhard, Applications of the discrete element method in mechanical engineering, *Multibody Syst. Dyn.* 18 (2007) 81-94.
[9] M. Nakano, T. Ando, Y. Nobusue and H. Kawamoto, Investigation on image profile of magnetic toner particles on photoreceptor in electrophotography, Japan Hardcopy 2004, (2004) 279-282.